Investigation of shape coexistence in ^{94}Mo, ^{96}Mo, ^{98}Mo and ^{100}Mo based on a two-dimensional model with the Bohr Hamiltonian

<u>Mardyban M.A.,</u>* *Kolganova E.A., Jolos R.V., Sazonov D.A., Shneidman T.M.

BLTP JINR

2021

Problem model

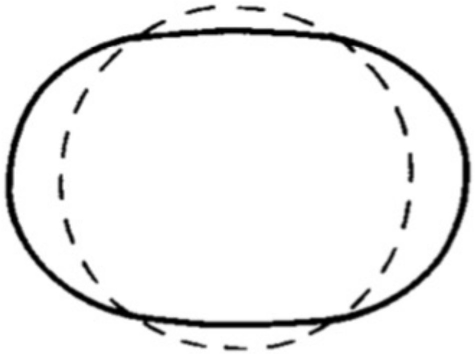

λ=2

λ=3

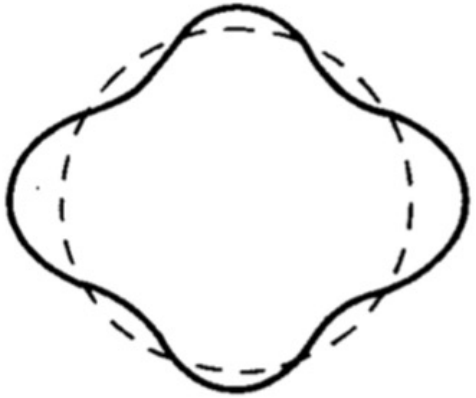

λ=4 $a_{40}>0$

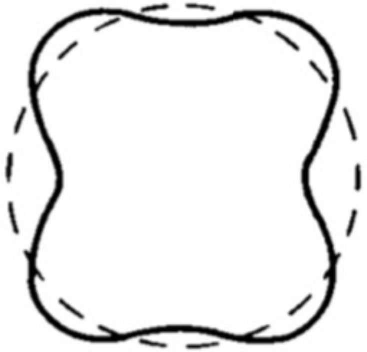

λ=4 $a_{40}<0$

$$R(\theta,\varphi) = R_0\left[1 + \sum_{\lambda=1} \sum_{\mu=-\lambda}^{\lambda} \alpha_{\lambda\mu}^{*} Y_{\lambda\mu}(\theta,\varphi)\right]$$

λ=2 (quadrupole); μ=-2,-1,0,1,2

$$\alpha_{21} = \alpha_{2-1} = 0, \quad \alpha_{22} = \alpha_{2-2}$$

$$\alpha_{20} = \beta\cos\gamma, \quad \alpha_{22} = \frac{1}{\sqrt{2}}\beta\sin\gamma$$

Nucleus shapes

Potential energy curves illustration.

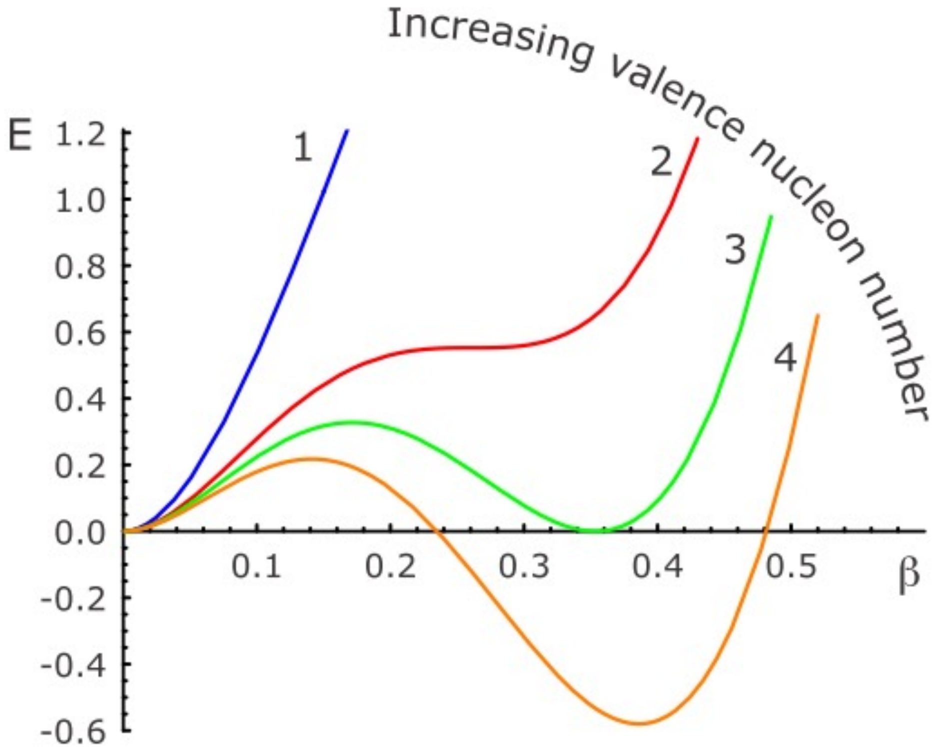

Spherical shape

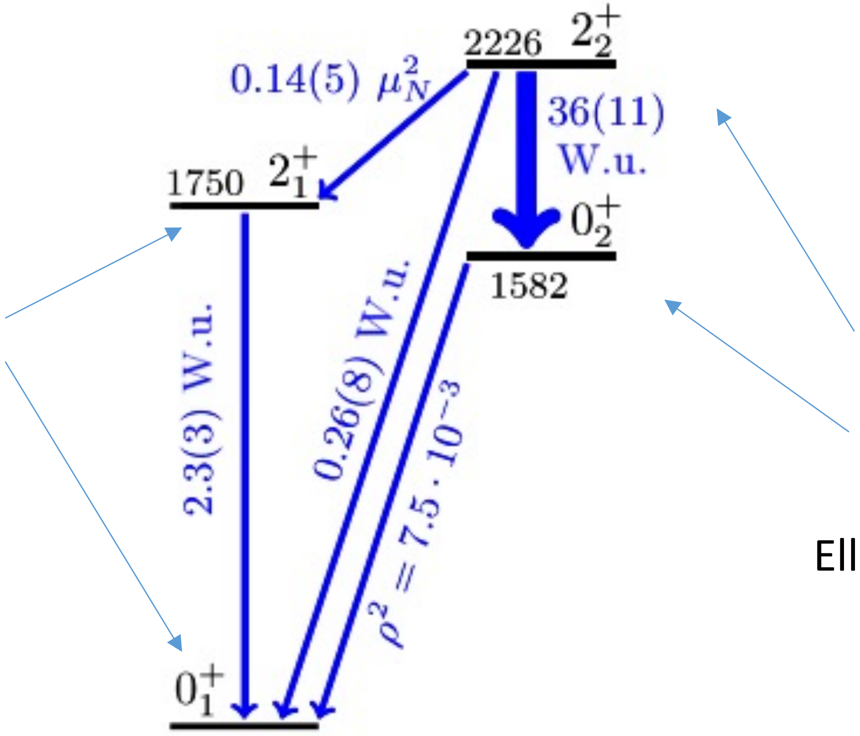

Ellipsoidal shape

- New experimental data: C. Kremer et al. "First Measurement of Collectivity of Coexisting Shapes Based on Type II Shell Evolution: The Case of ^{96}Zr" Phys. Rev. Lett. 117, 172503 (2016)

Bohr Hamiltonian

The collective quadrupole Bohr Hamiltonian can take the form:

$$H = -\frac{\hbar^2}{2B_0}\frac{1}{\sqrt{\omega r}}\frac{1}{\beta^4}\frac{\partial}{\partial\beta}\beta^4\sqrt{\frac{r}{\omega}}b_{\beta\beta}\frac{\partial}{\partial\beta} + \hat{T}_{\beta\gamma} + \hat{T}_{\gamma} + \frac{\hbar^2}{2B_0}\sum_k \frac{\hat{I}_k^2}{\Im_k} + V(\beta,\gamma)$$

$$w = b_{\beta\beta}b_{\gamma\gamma} - b_{\beta\gamma}^2, \quad r = b_1 b_2 b_3, \quad \Im_\kappa = 4b_\kappa\beta^2\sin^2(\gamma - \frac{2\kappa\pi}{3}).$$

The parameter B_0 is the overall dimensional scaling factor for the components of the tensor of inertia.
Coefficients $b_{\beta\beta}$ $b_{\gamma\gamma}$ and $b_{\beta\gamma}$ are dimensionless coefficients of inertia for β- and γ-oscillations.

Schrödinger equation that will be used to analyze the phenomenon of coexistence of forms:

Two-dimensional:

$$\left(-\frac{\hbar^2}{2B_0}\left[\frac{1}{\beta^4}\frac{\partial}{\partial\beta}\beta^4\frac{\partial}{\partial\beta}+\frac{1}{\beta^2\sin 3\gamma}\frac{\partial}{\partial\gamma}\sin 3\gamma\frac{\partial}{\partial\gamma}-\frac{1}{4}\sum_i\frac{I_i^2}{\beta^2\sin^2\left(\gamma-\frac{2\pi i}{3}\right)}\right]+V(\beta,\gamma)\right)\Psi=E\Psi$$

One-dimensional:

$$\left(-\frac{\hbar^2}{2B_0}\left[\frac{d^2}{d\beta^2}-\frac{1}{4\tau}\frac{d^2\tau}{d\beta^2}+\frac{3}{16}\left(\frac{1}{\tau}\frac{d\tau}{d\beta}\right)^2-\frac{\hat{\vec{I}}^2-\hat{I}_3^2}{3b_{rot}\beta^2}\right]+V(\beta)\right)\Psi=E\Psi$$

E2 transition

$$B(E2;\, 2_1^+ \rightarrow 0_1^+) = \frac{1}{5}\sum_\mu |< 2_1^+|Q_{2\mu}|0_1^+ > |^2$$

M1 transition

$$B(M1;\, 2_2^+ \rightarrow 2_1^+) = \mu_N{}^2\frac{9}{2\pi}|< 2_2^+|gR(\beta)|2_1^+ > |^2$$

One-dimensional model

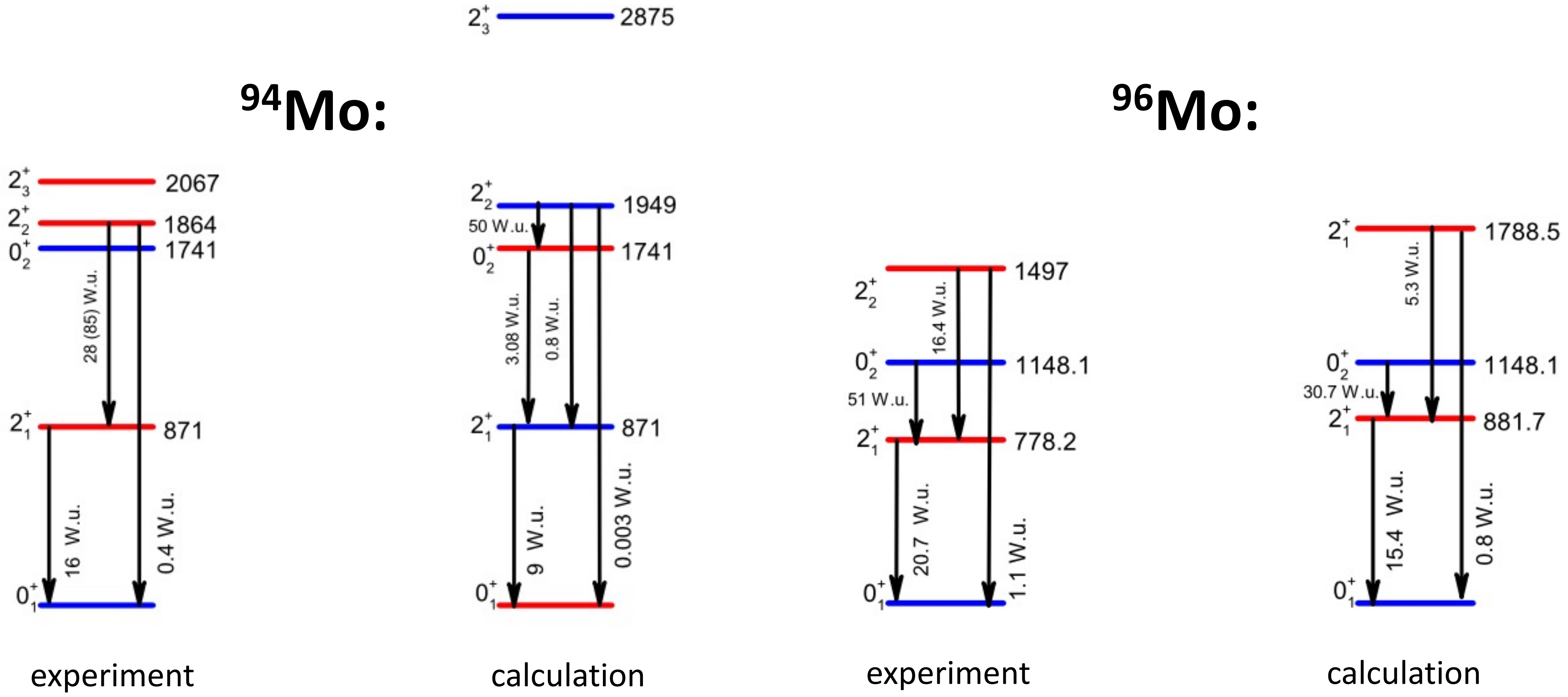

Potential energy V(β), calculated energies and wave functions for ^{94}Mo

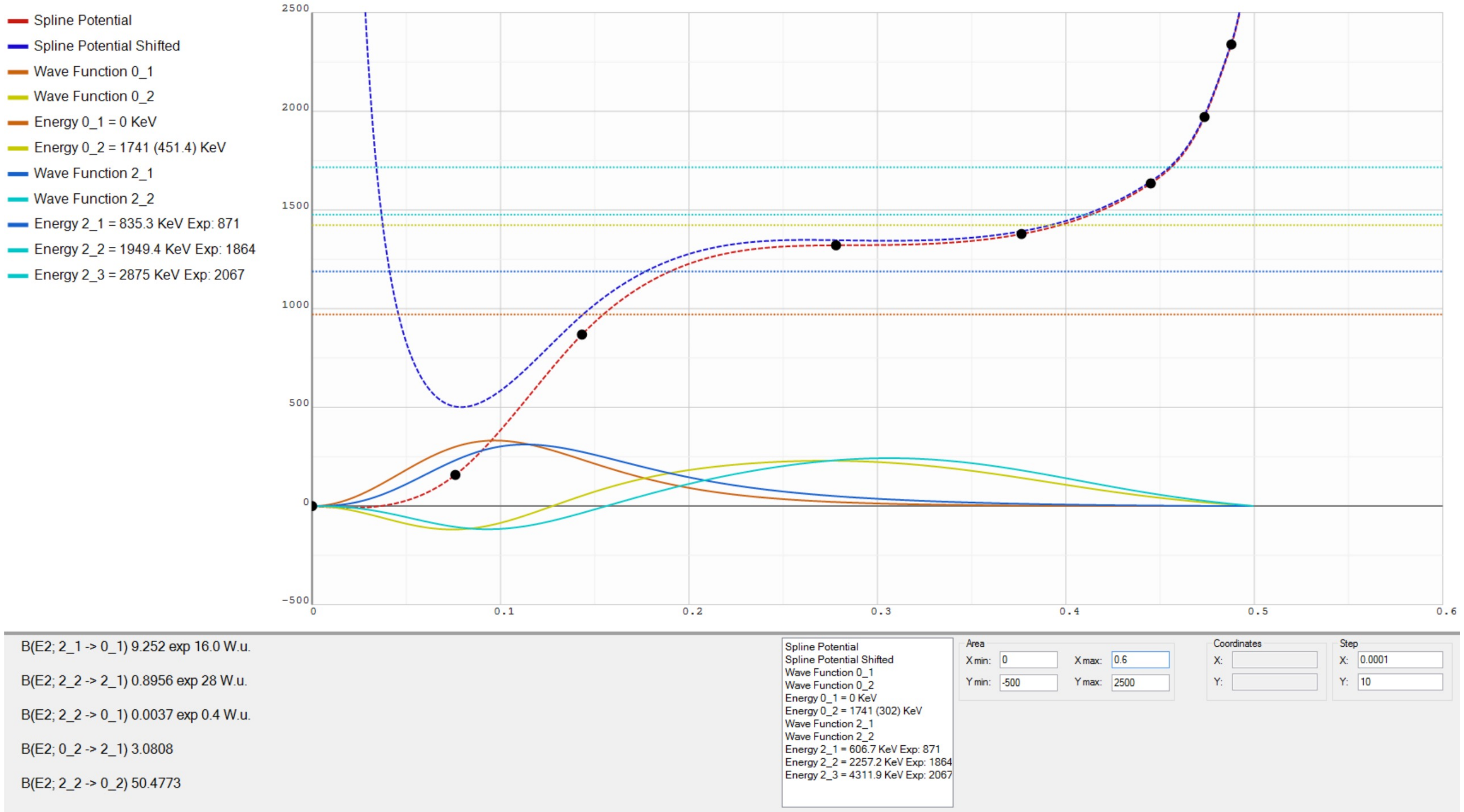

Two-dimensional model

Calculation results for ^{94}Mo

Energies and transitions	Experimental	One-dimensional	Two-dimensional
$E(0_2^+)$	1741	1741	1377
$E(2_1^+)$	871	835	857
$E(2_2^+)$	1864	1949	1631
$E(2_3^+)$	2067	2875	2301
$B(E2; 2_1^+ \to 0_1^+)$	16	9	13
$B(E2; 2_2^+ \to 2_1^+)$	28	0.9	29
$B(E2; 2_2^+ \to 0_1^+)$	0.4	0.004	0.13
-	-	$\chi_E^2 = 175$	$\chi_E^2 = 30$
-	-	$\chi_{B(E2)}^2 = 11.9$	$\chi_{B(E2)}^2 = 9.3$

Calculation results for ^{96}Mo

Energies and transitions	Experimental	One-dimensional	Two-dimensional
$E(0_2^+)$	1148	1148	1148
$E(2_1^+)$	778	881	778
$E(2_2^+)$	1498	1788	1446
$B(E2; 2_1^+ \to 0_1^+)$	20.7	15.4	14.4
$B(E2; 0_2^+ \to 2_1^+)$	51	30.7	59
$B(E2; 2_2^+ \to 2_1^+)$	16.4	5.3	32
$B(E2; 2_2^+ \to 0_1^+)$	1.1	0.86	0.36
-	-	$\chi_E^2 = 178$	$\chi_E^2 = 26$
-	-	$\chi_{B(E2)}^2 = 11.8$	$\chi_{B(E2)}^2 = 9.27$

Calculation results for ^{98}Mo

Energies and transitions	Experimental	Two-dimensional
$E(0_2^+)$	735	735
$E(2_1^+)$	787	795
$E(2_2^+)$	1432	1462
$E(2_3^+)$	1759	1796
$B(E2;2_1^+ \to 0_1^+)$	20.1	12
$B(E2;2_1^+ \to 0_2^+)$	9.8	9.7
$B(E2;2_2^+ \to 2_1^+)$	48	24
$B(E2;2_2^+ \to 0_1^+)$	1.02	0.26
$B(E2;2_2^+ \to 0_2^+)$	2.3	2.9
-	-	$\chi_E^2 = 14.6$
-	-	$\chi_{B(E2)}^2 = 11.3$

Calculation results for ^{100}Mo

Energies and transitions	Experimental	Two-dimensional
$E(0_2^+)$	695	695
$E(2_1^+)$	535	512
$E(2_2^+)$	1063	1072
$E(2_3^+)$	1463	1499
$E(4_1^+)$	1136	1106
$B(E2;2_1^+ \to 0_1^+)$	37.6	16.7
$B(E2;0_2^+ \to 2_1^+)$	89	44
$B(E2;2_2^+ \to 0_2^+)$	5.7	2.2
$B(E2;2_2^+ \to 2_1^+)$	52	28
$B(E2;2_2^+ \to 0_1^+)$	0.62	0.42
$B(E2;4_1^+ \to 2_1^+)$	69	36.7
$B(E2;2_3^+ \to 4_1^+)$	36	10
$B(E2;2_3^+ \to 0_2^+)$	15	13
-	-	$\chi_E^2 = 21.6$
-	-	$\chi_{B(E2)}^2 = 24.5$

Comparison of potential surface

^{94}Mo:

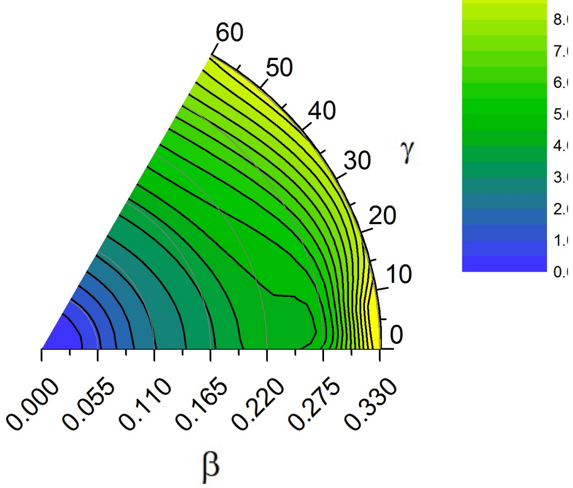

^{96}Mo:

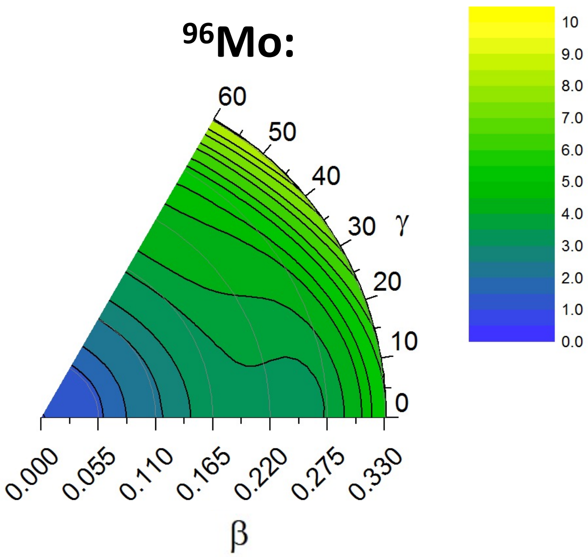

^{98}Mo:

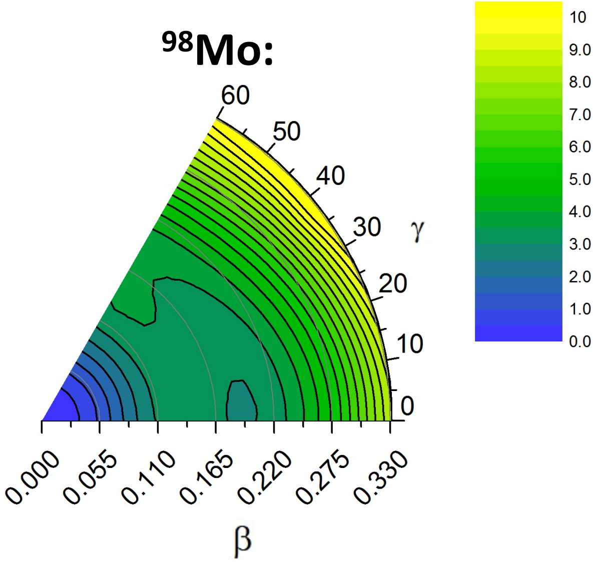

^{100}Mo:

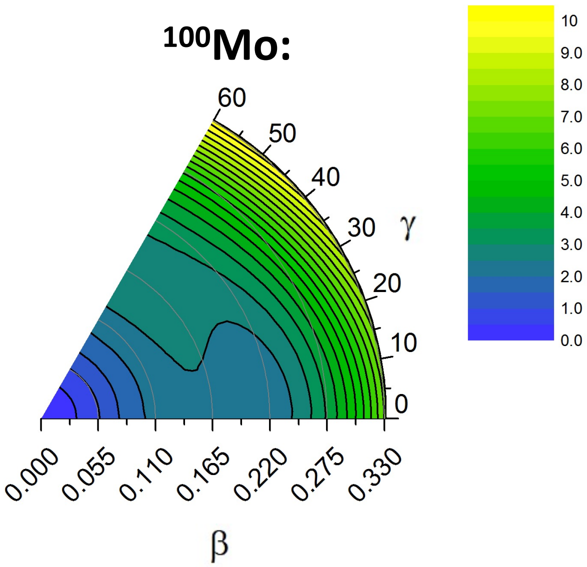

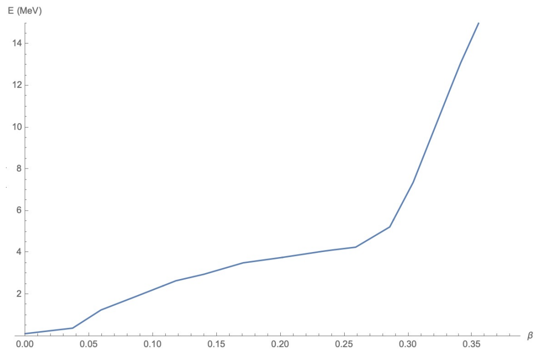

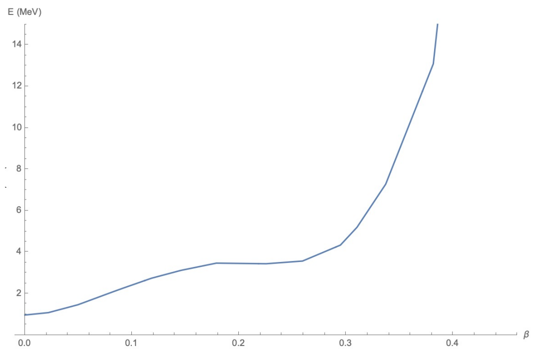

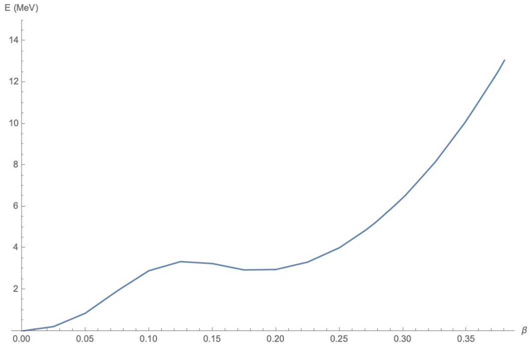

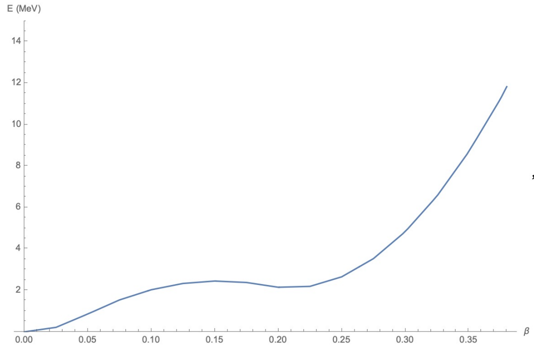

Conclusion

- The used model makes it possible to predict the probabilities of E2 transitions
- The obtained energies and transition probabilities of low-lying collective states are in good agreement with experiment

The main results are included in the articles:

D. A. Sazonov et al. Phys. Rev. C 99, 031304 (R) - (2019)
M.A. Mardyban et al. SNFP №6, 1960203 (2019)

Thank you for your attention!